Cerebral Cortex Advance Access published October 8, 2008

Cerebral Cortex
doi:10.1093/cercor/bhn178

The Organization of Orientation-Selective, Luminance-Change and Binocular-Preference Domains in the Second (V2) and Third (V3) Visual Areas of New World Owl Monkeys as Revealed by Intrinsic Signal Optical Imaging

Peter M. Kaskan, Haidong D. Lu, Barbara C. Dillenburger, Jon H. Kaas and Anna W. Roe

Department of Psychology, Vanderbilt University, 301 Wilson Hall, 111 21st Avenue South, Nashville, TN 37203, USA

Optical imaging was used to map patterns of visually evoked activation in the second (V2) and third (V3) visual areas of owl monkeys. Modular patterns of activation were produced in response to stimulation with oriented gratings, binocular versus monocular stimulation, and stimuli containing wide-field luminance changes. In V2, luminance-change domains tended to lie between domains selective for orientation. Regions preferentially activated by binocular stimulation co-registered with orientation-selective domains. Co-alignment of images with cytochrome oxidase (CO)–processed sections revealed functional correlates of 2 types of CO-dense regions in V2. Orientation-responsive domains and binocular domains were correlated with the locations of CO-thick stripes, and luminance-change domains were correlated with the locations of CO-thin stripes. In V3, orientation preference, luminance-change, and binocular preference domains were observed, but were more irregularly arranged than those in V2. Our data suggest that in owl monkey V2, consistent with that in macaque monkeys, modules for processing contours and binocularity exist in one type of compartment and that modules related to processing-surface features exist within a separate type of compartment.

Keywords: evolution, optical imaging, owl monkey, visual cortex, V2, V3

In the present experiments, we used optical imaging to reveal aspects of the functional organization of V2 (the second visual area) and V3 (the third visual area) in owl monkeys. Although V2 is an area common to most if not all mammals (Rosa and Krubitzer 1999), in primates it forms an elongated strip of cortex anterior to the border of V1 (Allman and Kaas 1974; Tootell et al. 1985; Stepniewska and Kaas 1996; Gattass et al. 1997; Lyon and Kaas 2002a). The distribution of V3 across mammals is less certain however, although it now appears that V3 likely exists in all primates (Kaas and Lyon 2001). Present understandings of the functional organization of V2 are rather extensive, with most results coming from either Old World macaque monkeys (DeYoe and Van Essen 1985; Hubel and Livingstone 1985; Peterhans and von der Heydt 1993; Roe and Ts'o 1995; Tootell and Hamilton 1989; Ts'o et al. 2001; Xiao et al. 2003; Wang et al. 2007; Chen et al. 2008) or New World squirrel monkeys (Livingstone and Hubel 1982; Tootell et al. 1983; Hubel and Livingstone 1985, 1987; Malach et al. 1994). In brief, there is evidence that V2 in these primates is subdivided into repeating sets of 3 functionally distinct types of stripe-like modules, often revealed with stains for the mitochondrial enzyme cytochrome oxidase (CO) (Wong-Riley 1979), that cross the width of V2. The 3 types of modules are usually referred to as thick, pale, and thin stripes, as they typically appear in brain surface views of brain sections processed for CO (Livingstone and Hubel 1983; Horton 1984; Tootell et al. 1985; Krubitzer and Kaas 1990a; Olavarria and Van Essen 1997; Sincich et al. 2003), although the 2 types of CO-dark bands are not consistently distinguishable as thick or thin (Tootell and Hamilton 1989; Krubitzer and Kaas 1990a; Levitt et al. 1994; Roe and Ts'o 1995). Thus, our usage of the terms "thick" and "thin" have become a functional term for stripes that exhibit preference for ocular integration and surface properties, respectively (Roe and Ts'o 1997). Despite these difficulties, much of the research effort has been in defining the functional properties of these 3 types of stripes. In V2 of macaque monkeys, most of the neurons in thick stripes are binocular and sensitive to horizontal disparities between the 2 eyes (Livingstone and Hubel 1987; Poggio et al. 1988; Peterhans and von der Heydt 1993; Roe and Ts'o 1995; Ts'o et al. 2001; Bakin et al. 2000). Recent optical imaging studies in macaque monkeys demonstrated that the thick stripes in V2 are more highly activated when both eyes were stimulated (Chen et al. 2008). As the binocular disparity-sensitive cells in the thick stripes require binocular stimulation, it seems reasonable that thick stripes would be more responsive to binocular stimuli than other stripes. The thick stripes also contain orderly representations of stimulus orientation (Malach et al. 1994; Ts'o et al. 2001; Xu et al. 2004). In contrast, the thin stripes in V2 of macaques are thought to represent surface properties of visual objects such as luminance and color (Tootell and Hamilton 1989; Roe and Ts'o 1995; Ts'o et al. 2001; Xiao et al. 2003; Wang et al. 2007). Luminance provides a basic cue for the percept of brightness and attribute commonly ascribed to surfaces. In macaque monkeys, the thin-stripe domains have been found to be responsive to changes in luminance (Wang et al. 2007). In addition, the thin-stripe domains have been shown to be sensitive to changes perceived by humans as changes in brightness (e.g., contrast effects), even when there was no physical change in luminance of the actual stimuli (Roe et al. 2005a). The question we had was if different stripe-like domains in V2 of owl monkeys (Fig. 1, Supplementary Fig. 1) are sensitive to binocular stimulation, and to luminance change, as the thick and thin stripes are in macaque monkeys.

New World owl monkeys, typically considered nocturnal (but see Wright 1994, for reports of daylight activity), have not shared a common ancestor with Old World macaque monkeys in approximately 40 million years. Similarities between macaque and owl monkeys would indicate that a type of functional organization of V2 has been retained in anthropoid primates for over 40 million years as the 2 lines adapted to quite different visual environments. Previous studies in owl monkeys indicate that they have dark and pale CO stripes as in other monkeys, but the dark stripes are often interrupted and sometimes fail to cross the width of V2 (Tootell et al. 1985; Krubitzer and Kaas 1990a). In addition, the stripes are not

always clearly thick and thin. Nevertheless, the thick stripes in V2 of owl monkeys resemble those of macaques in that they contain an orderly representation of stimulus orientation (Xu et al. 2004). Our present results indicate that different sets of CO bands in owl monkeys are selectively activated by binocular stimulation or by changes in luminance and that binocular- and luminance-sensitive domains appear to correspond to thick and thin stripes, respectively.

The other cortical area that we studied in these experiments was V3. Although the existence of V3 as a separate visual area or a visual area with dorsal and ventral halves corresponding to the lower and higher visual quadrants has been in question (for review, see Kaas and Lyon 2001), recent anatomical studies have provided clear evidence for a traditional V3 in owl monkeys as well as other primates (Lyon and Kaas 2002a, 2002b, 2002c). In owl monkeys, dorsal V3 is exposed on the dorsal surface of the brain next to V2, where it is accessible for optical imaging. Previous optical imaging studies in owl monkeys and prosimian galagos have provided evidence for orientation-specific domains in V3 that typically appear wider than those in V2 and a retinotopic organization that corresponds to that expected for V3 (Lyon et al. 2002; Xu et al. 2004). Here, we provide evidence for luminance-change and binocular preference domains, as well as orientation preference domains in V3.

Materials and Methods

In general, procedures followed those used previously (Kaskan et al. 2007). All procedures used in this study were approved by the Vanderbilt Animal Care and Use Committee and conformed to guidelines set out by the National Institutes of Health.

Animal Preparation

The 7 adult owl monkeys (*Aotus trivirgatus*) used in this study were initially given intramuscular injections of ketamine and atropine (10 mg/kg each) and were intubated and artificially ventilated with 2% isoflurane in oxygen. Anesthetic depth was continuously monitored by electroencephalography (EEG). End-tidal CO_2, heart rate, body temperature, and blood oxygen were also monitored continuously. Eyes were dilated with atropine sulfate and were refracted to focus on a computer screen, placed 24.5 cm from the animals' eyes. A craniotomy and durotomy were performed to expose the occipital lobe. The cortex was covered with agar and a clear glass coverslip to stabilize the brain. During imaging, the animal was maintained under a combination of sufentanil (2–4 μg/kg h), propofol (4–8 mg/kg h), and vecuronium bromide (0.05 mg/kg h). Values of propofol and sufentanil were adjusted within these ranges in order to keep the animal in a "surgical" plane of anesthesia (stage 3, plane 2).

Optical Imaging

Stimuli were generated with a Visual Stimulus Generation board (Cambridge Research Systems) and presented on a cathode ray tube monitor (Sony Trinitron, GDM F500R). The refresh rate was 100 Hz, well above the temporal frequency cut-off of owl monkeys (Jacobs et al. 1979). A Minolta CS-100 luminance meter was to measure the lowest luminance level of this monitor, which was 0.00 cd/m^2. Visual stimuli averaged 43 cd/m^2. Screen extent spanned about 70 × 56 degrees of visual field. In experiments that examined response to orientation and binocularity, electromechanical shutters were placed in front of the eyes to control monocular and binocular stimulations. The shutters were also used in some experiments to produce changes in luminance.

Images of reflectance change (intrinsic hemodynamic signals) corresponding to local cortical activity were acquired using Imager 3001 (Optical Imaging Inc, Germantown, NY) with 630-nm illumination (Roe and Ts'o 1995, Ramsden et al. 2001). Signal to noise ratio was enhanced by trial averaging (10–50 trials per stimulus condition) and by synchronization of acquisition with heart rate and respiration. Stimuli were presented for 5 s, during which 16–20 consecutive image frames were taken (4 Hz frame rate). Interstimulus interval for all stimuli was 8 s. Each frame contained 504 × 504 pixels (representing 8 × 8 mm cortex area). Stimuli were presented in blocks of randomly interleaved conditions. Stimulus onset and shutter opening for the respective eye occurred after the first 2 frames of imaging (0.5 s).

Visual Stimuli and Image Analysis

Orientation preference maps were acquired using full-screen, drifting, achromatic square-wave gratings with a mean luminance of 43 cd/m^2 and 100% contrast. Gratings drifted at 0.5 c/deg at 2 Hz and were of different orientations (0, 45, 90, and 135 deg). Orientation preference maps were generated from the binocular presentation of oriented gratings.

In order to reveal responses biased toward binocular stimulation, the 4 orientation conditions were presented to either both eyes simultaneously or to either the left eye or the right eye using eye shutters. Activity due to monocular stimulation was then subtracted from that due to binocular stimulation. The parameters used in generating monocular and binocular stimuli were the same as those used in generating orientation preference maps. We generated subtraction maps for orientation preference (e.g., 0–90 deg, 45–135 deg), binocularity (binocular conditions—monocular conditions) and luminance-change (temporal frequency—blank, or luminance-change conditions—luminance-sustained conditions).

In order to capture the responses of cells in the visual cortex that respond best to full-field luminance change, we used 2 methods. Luminance stimuli had no contour content and consisted of an even field of luminance. These binocularly presented stimuli were modulated either sinusoidally in time or with rapid onsets and offsets.

In one set of experiments, we sinusoidally modulated the luminance (100% contrast) of a wide-field stimulus at several different temporal frequencies (0.5, 1, 4, 8, and 16 Hz) around a mean luminance of 43 cd/m^2. To generate luminance-change maps, the activation resulting from a nonmodulated (steady state) blank screen of 43 cd/m^2 was subtracted from each modulated field of luminance. In another set of experiments, we used eye shutters to produce abrupt onsets and offsets of luminance. Four different stimulus conditions were presented. Two of these conditions contained changes in luminance and 2 did not. The 2 luminance-change conditions consisted of either the shutter opening or closing at the start of a trial (transient conditions). The 2 conditions that did not contain changes in luminance (sustained conditions) were created by either leaving the shutters open (43 cd/m^2, light sustained) or by leaving them closed (dark sustained). Single-condition luminance-change maps were generated by subtracting luminance non-modulated conditions (i.e., either light-sustained or dark-sustained conditions) from luminance-modulated conditions.

All results were initially first-frame subtracted using the first 2 frames in each trial. Maps were low-pass filtered with a Gaussian kernel of 3, 5, or 7 pixels, high-pass filtered with a Gaussian kernel of 80 or 120 pixels (1.27 or 1.9 mm) and clipped at 1 or 1.5 standard devaition from the mean using custom written software in Matlab. Signal strength scales and timecourses were generated with custom software in Matlab.

Histology and Border Placement

The animals were given a lethal dose of sodium pentobarbitol (80 mg/kg), and when the EEG showed no electrical activity, they were perfused transcardially with phosphate-buffered saline (PBS, pH 7.4), followed by 2% paraformaldehyde in PBS. After perfusion, the brain was removed and prepared for processing. The cortex was carefully removed from the underlying white matter, manually flattened (Krubitzer and Kaas 1990a), held between 2 glass plates, and stored overnight in 30% sucrose in PBS. The cortex was cut on a freezing microtome in sections parallel to the surface at a thickness of 100 μm (top 3 sections) and 50 μm (remaining sections). Sections were processed for CO (Wong-Riley 1979) to reveal architectonic borders and modular features of V2. Photographs of the histological material were taken with a digital camera (Nikon, DXM1200F) attached to a Nikon Eclipse E800 microscope. In some instances, photographs of CO-processed material were contrast-enhanced, leveled, high-pass

filtered, and blurred using Photoshop to make visualization of architectonic features more evident.

Several sources of information were used to identify the locations of the V1/V2 border and the V2/V3 border. The V1/V2 border, apparent on sections processed for CO, was identified by the location of CO blobs and was transferred to camera frames of interest (aligned as described below). This border closely corresponded to the V1/V2 border identified in optical imaging maps. Where adequate CO-stained material was unavailable, the optical imaging maps were used to identify the locations of the V1/V2 border, which was most apparent in binocular preference maps. The location of the V2/V3 border was estimated from previous estimates of the width of V2 at this eccentricity (approximately 4 mm, Lyon et al. 2002; Lyon and Kaas 2002a) and from the optical imaging maps, where orientation preference domains in V3 are known to join into regions wider than orientation preference stripes in V2 (see Xu et al. 2004).

Alignment Methodology

Images of the tissue were aligned to images of the surface vasculature taken in vivo with the imaging camera. Figure 2 is an example of these procedures (see also Supplementary Fig. 2) Figure 2*A* is an image of the surface vasculature of the visual cortex of owl monkey 07-46, taken in vivo with the optical imaging camera under green (570 nm) illumination. The same field of view was used during optical imaging procedures. The superficial vasculature seen in a CO-stained superficial section (Fig. 2*B*) aligns well with the cortical vasculature seen in vivo (Fig. 2*A*), as demonstrated by the blood vessels that have been traced from the in vivo image (Fig. 2*A*) and overlaid upon the superficial CO-stained section (Fig. 2*B*). Adobe Photoshop was used to align the histological sections with the optical imaging camera frames. In some instances, "stretching" was required in addition to scaling and rotating images to account for minor irregularities due to curvature of the brain in vivo, flattening the cortex and mounting the CO-processed tissue on slides. Deeper sections of the flattened cortex, like that shown in Figure 2*C* were aligned with more superficial sections by using radially oriented blood vessel lumens. In Figure 2*B,C*, several of these radially oriented vessel lumens are indicated with black arrows. Optical imaging maps (such as the orientation map shown in Fig. 2*D*) are therefore in register with CO-processed sections of the cortex (note: vascular artifacts in Fig. 2*D* match large vessels in superficial CO section in Fig. 2*B*, as shown with vessel overlay).

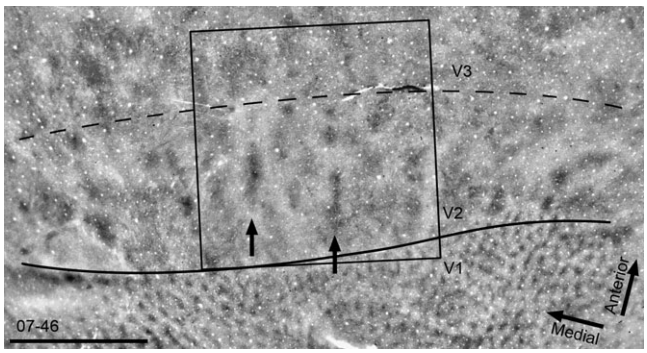

Figure 1. Irregular CO stripes in V2. A flattened section of the visual cortex from owl monkey 07-46, stained for CO revealed the borders between V1 and V2 (solid line) and between V2 and V3 (dashed line). In V1, a pattern of CO blobs was evident. In V2, larger irregular CO-dark bands or stripes running roughly perpendicular to the V1/V2 border were present. Two thinner CO-dense regions are indicated with arrows. The large box represents the 8 × 8 mm field of view centered over V2 shown in Figures 2 and 4. Scale bar: 5 mm.

Results

We used intrinsic signal optical imaging to examine the functional organization of the second (V2) and third (V3) visual areas in 7 adult owl monkeys (*A. trivirgatus*). Modular patterns of activation were present in V2 and V3 in response to visual stimulation. Table 1 lists the cases examined for orientation preference, luminance-change, and binocular preference domains in V2. We report for the first time the presence of domains in V2 and V3 of owl monkeys that correspond to changes in full-field luminance and domains exhibiting preference to stimulation of both eyes versus one eye. Maps of orientation preference in V2 were present in every case, and they were related in systematic ways to the locations of luminance-change domains and domains biased to respond to binocular stimulation. In V3, these relationships were less regular. In the following sections, we describe orientation preference, luminance-change domains, and binocular preference domains in V2 and V3, and in V2 relate the locations of these domains to CO preparations of the flattened neocortex. We did not find any relationship between CO architecture and optically imaged domains in V3. The 3 figures presented below are organized in a similar manner, with 3 optical imaging maps presented first, followed by a section stained with CO, where available, and finally a summary panel demonstrating the relationships between the optical imaging maps and the CO-stained cortex. Despite the high degree of interindividual variability in CO expression in V2, the organization of V2 for luminance-change and binocularity corresponded well with patterns of CO expression.

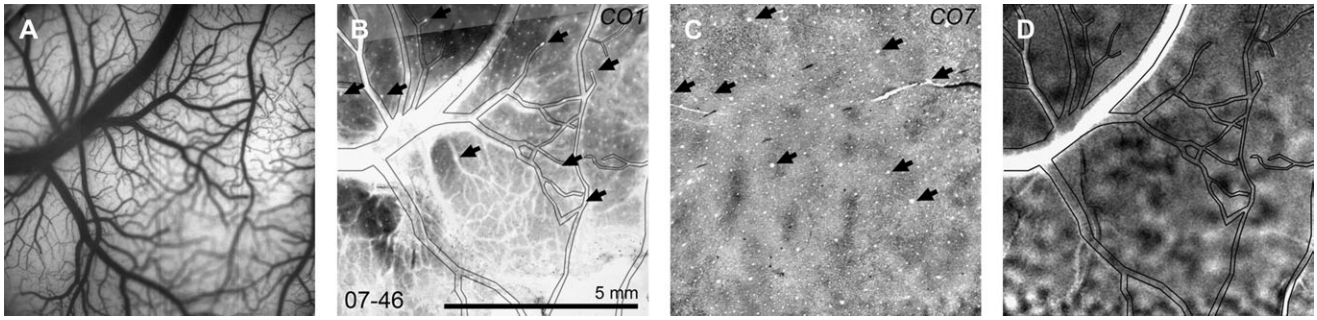

Figure 2. Alignment method. The panels in this figure demonstrate the procedures used to align flattened sections of the visual cortex to the optical imaging camera frame. Each panel corresponds to the boxed region shown in Figure 1. In *A*, an image of the surface vasculature taken with the imaging camera in vivo is shown. Panel *B* is the most superficial CO-stained section. Blood vessels from panel *A* have been outlined and are shown overlaid on panel *B*. Panel *C* is a photograph of a CO-stained section approximately 500 μm deep. Radial blood vessels used for alignment are indicated with arrows in *B* and *C*. Panel *D* is a horizontal–vertical orientation preference map; the blood vessel pattern traced from panel *A* is included. Blood vessel patterns in *A, B*, and *C* were used to align the CO-processed sections with the imaging frames. Scale bar: 5 mm.

Orientation Response

In each owl monkey, we measured changes in cortical reflectance in response to the presentation of full-screen drifting gratings of 4 orientations, where movement of the grating was perpendicular to the orientation of the grating. Figure 3*A* illustrates a typical reflection pattern seen when the responses to horizontal gratings were subtracted from those of vertical gratings. Horizontal preferring domains are represented by darker pixels; vertical preferring domains are represented by lighter pixels. By obtaining this type of orientation preference map, we were able to estimate the anterior and posterior borders of V2, based on the rostrocaudal extent of orientation domains, which were congruent with previous estimates (Lyon et al. 2002; Xu et al. 2004) of the rostrocaudal width of V2 at this eccentricity (approximately 4 mm). Borders were later confirmed by alignment with sections stained for CO. Orientation preference maps from other cases are shown in Figures 4*A*, 5*A*, and 6*A*.

Similar to previously described orientation domains in owl monkeys (Xu et al. 2004), orientation preference domains were smallest in V1 and larger in V2 and V3. In V1, orientation preference domains were found throughout its extent. In V2, orientation preference domains were noticeably larger and sometimes clustered to form stripes alternating with regions lacking orientation preference domains. Although the stripe organization is less evident in this case, in other cases (e.g., Fig. 4*A*), the stripe organization of orientation response in V2 is quite clear. We termed these regions orientation-responsive stripes, or OR stripes. Orientation preference domains were also present in V3 (Figs 3*A*–6*A*). As in V2, orientation preference domains in V3 were interrupted by zones lacking orientation preference (arrow, Fig. 3*A*).

We examined the temporal response of reflectance change in owl monkeys due to the presentation of oriented gratings to gauge whether this response was similar to that observed in other primates and to compare it to the timecourse and signal strength of response to luminance modulation (see below). Figure 3*B* shows the timecourse of reflectance change for the small "superpixel" (white box in Fig. 3*A*) centered over a horizontal preferring domain (0 deg) in V2. Changes in reflectance over a period of 5 s of stimulation are shown (4 frames/s). Similar to intrinsic signals recorded in anesthetized macaque monkeys, the magnitude of maximal reflectance change ranged from about 0.1–0.2%. The magnitude of this signal also varied with the orientation preference of the recorded domain. The greater response for the superpixel measured in Figure 3*A* was obtained with horizontal (0 deg) gratings (solid line), with a weaker response observed for 90-degree gratings (dotted line).

Table 1
Summary of cases examined

Case	OR stripes	Orientation preference domains	Luminance-change domains	Binocular domains	CO histology	Figure
05-14	+	+	+	Not tested	Good	
05-41	+	+	Weak	Not tested	Poor	
06-28	Weak	+	+	+	Poor	
06-38	+	+	Weak	Not tested	Poor	
06-59	Weak	+	Absent	+	Good	
07-37L	+	+	+	+	Good	4
07-37R	+	+	+	+	Good	5
07-46	+	+	+	+	Good	6

Note: We examined visual cortex in 7 adult owl monkeys. Most cases demonstrated the presence (+) of luminance-change domains, binocular domains, and orientation preference domains in V2. Those that exhibited good CO staining are shown in Figures 4 and 6.

Orientation Preference, Luminance Modulation, and Binocular Preference Response in V2

In addition to oriented gratings, 2 types of stimuli that have not previously been used in owl monkeys revealed additional aspects of the functional organization of V2. In macaque monkey V2, binocular preference domains colocalize with thick stripes (Roe and Ts'o 1995; Ts'o et al. 2001; Roe et al. 2007; Chen et al. 2008) and regions preferentially responsive to full-field luminance change colocalize with thin stripes (Roe et al. 2005a). In owl monkeys, responses to luminance modulation, to binocular minus monocular stimulations and to luminance change were examined. In most cases examined (Table 1), a clear spatial relationship between luminance-change domains, binocular domains, CO stripes, and domains selective for orientation was evident. In the following 3 figures (Figs 4–6), results from 3 cases are presented that demonstrated the presence of these domains and their relationship with CO-stained cortex.

In the first case (Fig. 4), 3 optical imaging maps are shown (case 07-37L) along with the corresponding region of visual cortex stained for CO. The locations of the borders were based

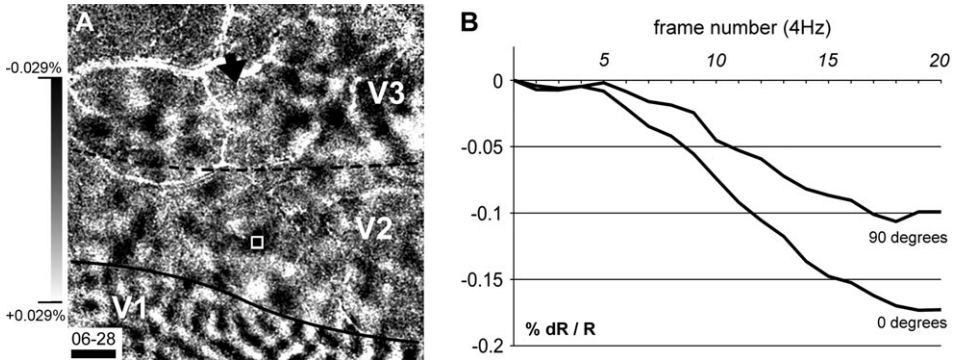

Figure 3. Orientation preference map and timecourse. In panel *A*, an acute-oblique orientation preference map is shown for owl monkey 06-28. The camera frame is 8 × 8 mm. The approximate borders between V1 and V2 (solid line) and between V2 and V3 (dotted line) are indicated. The white box indicates a superpixel placed within a horizontal (0 deg) orientation domain within V2. The black arrow indicates a portion of V3 that lacked orientation preference domains. Percent signal change for the map shown in panel *A* is shown to the left of *A*. The signal strength (% change in reflectance) from the superpixel indicated in *A* for 0 and 90 deg orientations is shown in panel *B* during a 5-s period of stimulation (4 Hz frame rate) with drifting gratings. Numbers at the top of the timecourse data in *B* indicate frame number. Scale bar: 1 mm.

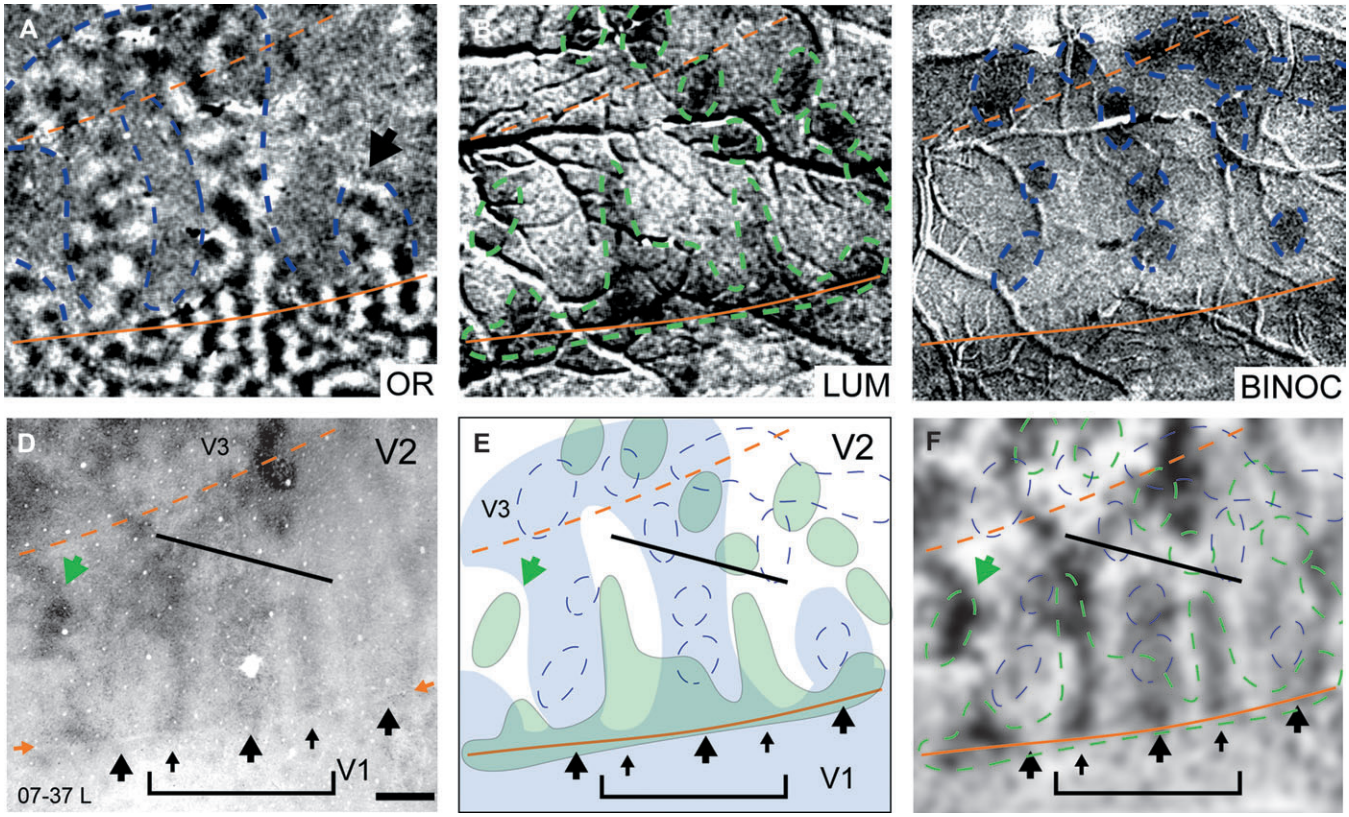

Figure 4. Orientation, luminance-change, and binocular domains in V2 and V3, and their relationship to CO-dense stripes in case 07-37L. An acute-oblique orientation preference map is shown in *A*. The borders between areas V1 and V2 (solid lines) and between V2 and V3 (dashed lines) are shown in orange. Stripes of well-organized orientation preference (OR stripes) are indicated with blue-dashed lines in V2. Two OR stripes ran across the extent of V2 and joined with a region of V3 containing OR domains. The OR stripe on the right stopped short of the V2/V3 border (black arrow). In *B*, a map of luminance change is shown (see Materials and Methods), and luminance-change domains in V2 and V3 are indicated with green-dashed lines. Panel *C* shows a binocular–monocular imaging map; binocular domains in V2 and V3 are highlighted with blue-dashed lines. In a section stained for CO, *D*, alternating CO-thick (large arrows) and CO-thin stripes (small arrows) are apparent. The hole in the center thick stripe is the site of an injection of anatomical tracer. The V1/V2 border is indicated with 2 small orange arrows. In *E*, a diagram showing the relative locations of OR stripes (blue shading), luminance-change domains (green shading), and binocular domains (blue dashed lines) is shown. Binocular domains coregistered with OR stripes in V2 and V3. In V2, luminance-change domains (light green shading) occupied regions of V2 adjacent to OR stripes and binocular domains (blue shading and blue-dashed lines, respectively). In V3, luminance-change domains and binocular domains were found within regions containing orientation preference domains, but luminance-change domains and binocular domains were found to occupy adjacent regions of V3. In *F*, luminance-change domains and binocular domains are shown in relation to a "filtered" (see Materials and Methods) CO-processed section of visual cortex. CO-thick stripes (wide arrows, panels *E, D*, and *F*) coregistered with orientation preference domains and binocular domains, and CO-thin stripes (narrow arrows) coregistered with luminance-change domains. This relationship was most obvious within the bracketed region (panels *E, D*, and *F*); note the correspondence between the optically imaged domains and the CO architecture, indicated between the brackets and the black line in panels *E, D, and F*. The green arrow in panels *D, E*, and F indicates the location of luminance-change domain and a corresponding CO-dense spot in V2. Scale bar: 1 mm.

upon sections stained for CO, from previous estimates of the width of V2 at this eccentricity and from the optical imaging maps (see Materials and Methods). As previously reported, orientation preference domains in owl monkeys typically formed stripes that were oriented across the anterior-posterior extent of V2 (regions within blue dotted lines in Fig. 4*A*). The orientation-responsive (OR) stripes in this case were approximately 1.5 mm thick. Most OR stripes were about 3–5 mm long and stretched across V2 from the posterior border with V1 to the anterior border with V3. Regions of V2 between the OR stripes did not contain orientation-responsive domains. In some owl monkeys, we have observed OR stripes that stop short of the V2/V3 border. Although we cannot rule out the possibility of a weak cortical signal, in this case, one stripe (indicated with an arrow on the right side of Fig. 4*A*) appeared shorter than the others.

Luminance-modulated domains in V2 were also revealed in this case. Eye shutters placed in front of both eyes were simultaneously opened and closed to reveal a neutral gray screen (43 cd/m^2) in order to create binocular onsets and offsets in luminance. Conditions not containing changes in luminance ("blanks," sum of images obtained with shutters open throughout imaging period plus those obtained with shutters closed throughout imaging period) were subtracted from conditions containing luminance change (sum of closed-to-open and open-to-closed conditions) to create a luminance modulation map (see Materials and Methods). In Figure 4*B*, luminance-modulated domains are indicated by green dashed lines. The long axis of some of these luminance-modulated domains was oriented perpendicular to the V1/V2 border. Other luminance-change domains appeared as patches or beads strung together across the anterior-posterior extent of V2. Some of the patch-like domains in this case formed extensions of the more stripe-like or oval-shaped domains that originated from the V1/V2 border. In this case, the overall impression was one of luminance-change stripes that ran from the V1/V2 border to the V2/V3 border in a beaded or patch-like manner.

Preferential responses to binocular stimulation were also apparent in V2. Domains preferring binocular stimulation

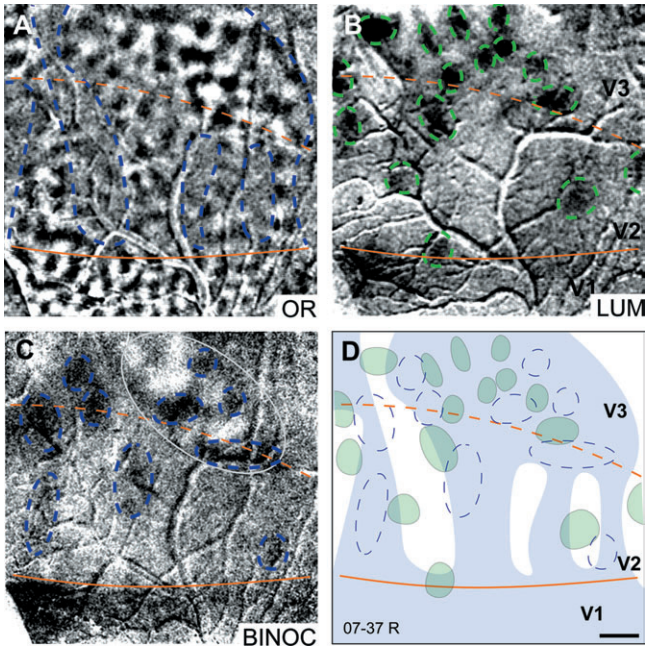

Figure 5. Orientation and luminance-change domains in V2 and V3 in case 07-37R. An acute-oblique orientation preference map is shown in *A*. The borders between areas V1 and V2 (solid lines) and between V2 and V3 (dashed lines) are shown in orange. In V2, regions of well-organized orientation preference (OR stripes) are indicated with blue-dashed lines. OR stripes in V2 were coextensive with regions of V3 (also indicated with blue-dashed lines) containing orientation preference domains. In *B*, a map of luminance change is shown, where luminance-change domains are circled with green-dashed lines in V2 and V3. In *C*, a binocular–monocular map demonstrated the presence of binocular preferring domains, circled in blue in V2 and V3. The light gray oval indicates a "zebra stripe-like" region in V3 that includes alternating binocularly biased domains. In diagrammatic form in *D*, orientation-preference domains are indicated with blue shading, binocular preferring domains are circled in blue, and luminance-change domains are indicated in green. In V2, binocular domains were found within regions containing orientation preference domains that were adjacent to luminance-change domains. In V3, luminance-change domains occupied regions of cortex adjacent to binocular domains. Each panel is 8 × 8 mm. Scale bar: 1 mm.

(Fig. 4*C*) were revealed by subtracting the activity to monocular stimulation from that to binocular stimulation (see Materials and Methods). Binocular preference domains were oval in appearance and formed patches that ran together into stripes or bands across the anterior-posterior extent of V2, similar in extent to the luminance-change domains shown in Figure 4*B*. The majority of binocular preference domains (Fig. 4*C*) co-registered with the locations of OR stripes (Fig. 4*A*) and largely avoided regions of V2 occupied by luminance-change domains (Fig. 4*B*). These relationships are represented schematically in Figure 4*E* (light blue: orientation, green: luminance, dotted blue outlines: binocular). The stripe-like organization and patchiness of these domains was apparent and gave the impression of an anterior to posterior organization.

We related the imaging results to the patterns of CO-dense stripes in V2. In Figure 4*D*, a flattened CO-stained section revealed the borders between V1 and V2 and demonstrated the presence of CO-dense stripes in V2. The CO-dense stripes in this case were mottled and patchy; one varied in width and appeared to merge with a neighboring CO light region (see small arrow, left thin stripe, Fig. 4*D*). In some portions of V2 in this case, the CO-dense stripes were relatively thick (thick black arrows) or thin (thin black arrows) and were oriented perpendicular to the V1/V2 border. The bracketed region is most characteristic of CO thick and thin stripes. The stripe-like patterns and patchiness of CO label in V2 is mirrored by the organization of luminance-change domains, binocular domains, and OR stripes.

In the diagram shown in Figure 4*E*, the large arrows indicating CO thick stripes point toward OR stripes containing binocular domains. The 2 thin-stripe arrows indicate adjacent luminance-change domains whose long axis is oriented perpendicular to the V1/V2 border. Regions of V2 that were occupied by OR stripes (shown in blue shading) and binocular domains (shown in blue dashed lines) tended to avoid those areas of V2 that contained luminance-change domains (shown in green shading).

Further examination revealed a good degree of correspondence between CO staining and luminance-modulated domains (Fig. 4*F*). For instance, in the left-most thin stripe, 2 domains of strong luminance modulation overly 2 domains of strong cytochrome staining (indicated by green arrow). The middle thin stripe co-localizes with a portion of the luminance-change region (outlined by green dotted line). The rightmost thin stripe also largely co-localizes with the luminance-change activation, the lower portion of which stops short of reaching the V2/V3 border. In the bracketed region of Figure 4*F*, the 2 thin stripes (indicated with thin arrows) co-registered with luminance-change domains (indicated with green dashed lines). The thin stripes defined by CO architecture (Fig. 4*D*, see also Supplementary Fig. 3) seemed to stop short of reaching the V2/V3 border, indicated with a solid black line. This line also indicates the location within V2 where these luminance-change domains ended, short of the V2/V3 border (Fig. 4*F*). Note that the thick stripe between these 2 thin stripes (thick arrow, Fig. 4D) also seemed to stop short of the V2/V3 border and at a point that corresponded to the location of 2 binocular preference domains. Thus, although the relationship between luminance modulation and thin cytochrome stripes is not one-to-one, there are still some striking correspondences. The domains imaged in this case and their relationships to CO-architecture were common to the owl monkeys we examined (see Table 1). In the sections that follow we present 2 additional cases.

Similar results were obtained in a second case (Fig. 5). Modular patterns of visually evoked activation were present in V2, and these activity patterns were related to each other in systematic ways. As in the previous case, orientation stripes were revealed in V2 of case 07-37R. Figure 5*A* illustrates an orientation map with 4 OR stripes in V2 (blue dashed lines). These stripes were oriented roughly perpendicular to the V1/V2 border. Each stripe ran from V1 to V3 without interruption; the several joining OR stripes in V2 appeared to merge into a large region of orientation preference in V3. Although OR stripes in this case seemed thinner than others, the overall OR stripe width in this case was approximately 1 mm. Luminance-change domains were also observed in case 07-37R (Fig. 5*B*). Between the OR stripes were regions of V2 that did not contain orientation-responsive domains. As in the previous case, luminance modulation was produced by using eye shutters (see Materials and Methods) to create luminance onsets and offsets. Luminance-change domains are circled in green dashed lines. In this case, luminance-change domains did not seem to form obvious stripes across the anterior-posterior extent of V2. Rather, they formed oval-shaped domains within V2. Finally, the locations of domains more activated during binocular stimulation are shown in Figure 5*C*. The binocular domains in this case

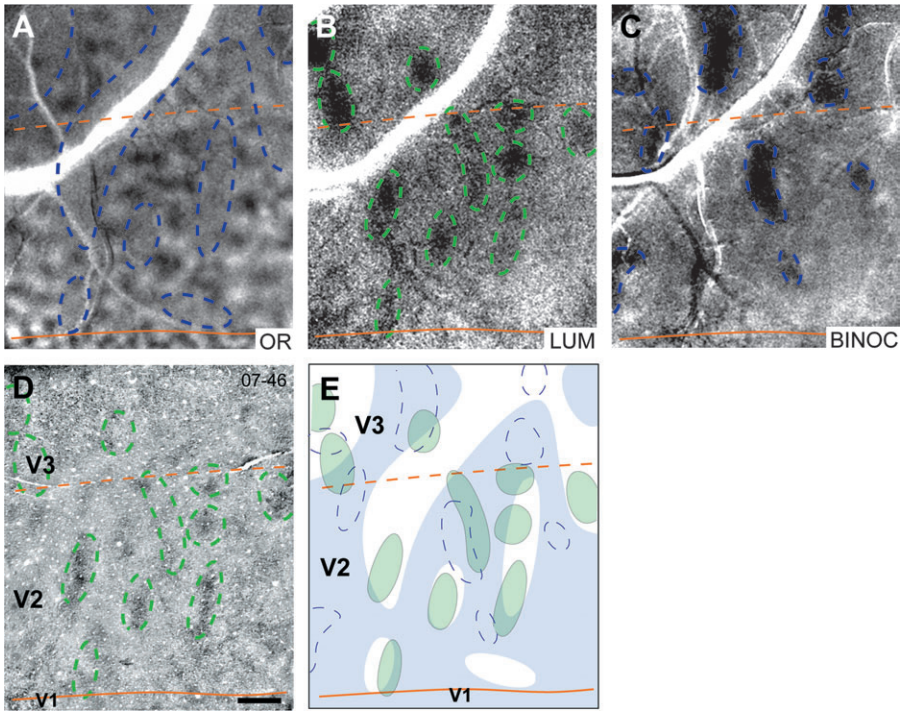

Figure 6. Orientation, luminance-change, and binocular domains in V2 and V3 and their relationship to CO-dense stripes in case 07-46. In *A*, an acute-oblique orientation preference map is shown; the borders between areas V1, V2, and V3 are indicated in orange. Orientation domains in V2 clustered to form stripes (blue-dashed lines) that were continuous with orientation domains in V3. In V2, gaps or spaces in the map of orientation preference were evident (circled, blue-dashed lines). The blue-dashed lines distinguish regions with orientation-selective domains from those without. In *B*, a map of luminance change is shown; luminance-change domains, present in V2 and V3, are indicated with green-dashed lines. In *C*, binocular domains were apparent within V2 and V3 (blue-dashed lines). In *D*, a section stained for CO revealed CO-dark regions that appeared as spots or ovals in V2; the borders of luminance-change domains (marked with green-dashed lines) are shown in relation to the CO section. Several luminance-change domains indicated with green-dashed lines in *B* corresponded to CO-dense regions in V2. In *E*, a diagram showing the relative locations of OR stripes (blue shading), binocular domains (blue-dashed lines), and luminance-change domains (green-dashed lines) in V2 and V3 is shown. Scale bar: 1 mm.

appeared oval shaped, the long axis of which ran perpendicular to the V1/V2 border.

A diagrammatic representation of each of the optical imaging maps is shown in Figure 5*D*. Binocular domains (blue dashed lines) largely overly regions of orientation preference (light blue regions) and, in V2, luminance-change (green domains) domains largely avoid regions of orientation preference.

Similar patterns of visually evoked activity were present in a third case. In Figure 6*A*, a map of orientation preference is shown. Orientation-responsive domains were apparent in V2 along the V1/V2 border, but this case exhibited weaker stripe-like organization. More anteriorly within V2, OR stripes merged and ran into V3. Because of the lack of clear stripes, it was difficult to discern the width of OR stripes. Between OR stripes, there were obvious regions that did not exhibit prominent orientation responsiveness. These regions appeared as holes or breaks in the OR map. The blue dashed lines in Figure 6*A* distinguish regions with orientation-selective domains from those without. Figure 6*B* shows a map of luminance modulation. The stimulus used in this case is different from the luminance modulation stimulus used in Figures 4 and 5. This map is a subtraction of activation due to a full-field luminance stimulus sinusoidally modulated (4 Hz) minus an unmodulated blank control of equal average luminance. In this case, luminance-change domains appeared round or elongated. The axis of elongated luminance-change domains was oriented roughly perpendicular to the V1/V2 border as in previous examples. The locations of binocular domains are shown in Figure 6*C* and are circled in blue dashed lines. The binocular domains in this case appeared oval shaped, the long axis of which ran perpendicular to the V1/V2 border. In this case, one binocular domain appeared much larger than the others and measured approximately 700 μm × 2 mm. Other binocular domains in this case ranged in size from about 300–600 μm wide and 800 μm to 1.5 mm long and were similar in size to those in other cases (see Figs 4 and 5).

In Figure 6*D*, the corresponding region of the visual cortex stained for CO is shown. In this section, CO-dense regions were apparent, and there was some impression of a stripe-like pattern across the width of V2, where the darkest CO-dense regions appeared thin. When the luminance-change domains shown in B were aligned with this CO-stained section of the visual cortex, it was apparent that the majority of luminance-change domains (green dotted lines) corresponded with the thinner CO-dense regions of V2.

The diagram in Figure 6*E* illustrates the relative locations of luminance-change domains (green domains), binocular domains (blue dashed lines), and OR stripes (light blue domains). Again, binocular domains (blue dashed lines) largely overlay regions of orientation preference (light blue regions), and, in V2, luminance-change (green domains) domains largely avoid regions of orientation preference.

Intrinsic Signal Timecourse Related to Luminance Modulation in V2

To further convince ourselves that these luminance domains were not artifactual, we examined cortical response to luminance modulation presented at different temporal

frequencies. Because cortical neurons are known to have different temporal frequency tuning curves, the response magnitude of the intrinsic signal should vary with the population temporal frequency preference. Furthermore, we predicted that if these luminance domains are true domains that their location should remain constant regardless of temporal frequency optimality. To address these predictions, we used a temporally varying uniform field of luminance that oscillated sinusoidally at frequencies ranging from 0.5 to 16 Hz. We chose this range of temporal frequencies because these values span those that have been shown to activate single neurons in V1 of owl monkeys (O'Keefe et al. 1998) and V2 of macaque monkeys (Levitt et al. 1994). The majority of neurons in V2 were responsive to frequencies ranging from 4 to 8 Hz, with fewer neurons responding to frequencies above or below this range (Levitt et al. 1994). In V1 of owl monkeys, the temporal frequency preferences of cells in superficial layers were significantly lower than in deeper layers (O'Keefe et al. 1998), suggesting that there may also be layer-specific differences in temporal response. We predicted 2 results. First, we expected that, at the locations of the luminance-change domains, we should obtain significant reflectance changes within the 0.5–16 Hz range. Second, given that the imaged response results from an integration of a population of neurons, that neurons responsive to wide-field luminance change tend to be tuned to lower temporal frequencies and that nocturnal animals such as the owl monkey may have visual systems optimized for lower contrasts and lower temporal frequencies, we predicted that the optimal temporal frequency of the optical signal would be similar or lower than the published single unit optimum (in macaque thick (4.1 Hz), thin (2.8 Hz), and pale (3.2 Hz) stripes (Levitt et al. 1994) and in owl monkey V1 (3 Hz) (O'Keefe et al. 1998)).

In Figure 7, 5 luminance modulation maps are presented (same case as shown in Fig. 6). Each map is a subtraction map and represents the activation due to a given temporal frequency of full-field sinusoidal modulation minus a blank condition (see Materials and Methods). Temporal frequencies of 0.5, 1, 4, 8, and 16 Hz are shown in Figure 4*A–E*, respectively. These maps revealed that, as predicted, each of these temporal frequencies produced significant optical response and that the locations of luminance-modulated domains are constant across different temporal frequencies of modulation, demonstrating localization of luminance-modulated response to these domains. In addition, luminance-modulated domains appeared

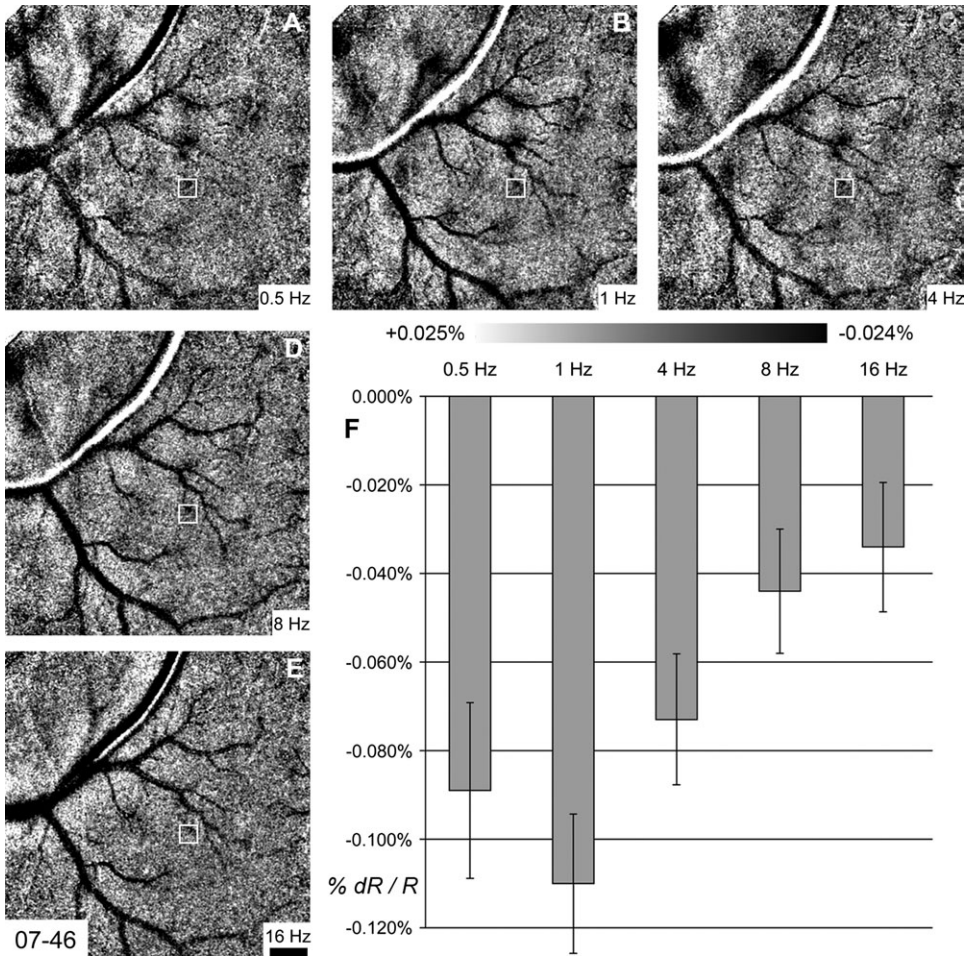

Figure 7. Signal strength related to luminance modulation. Five luminance-change maps taken from the boxed region shown in Figure 1 are displayed. Each panel is a map of sinusoidally varying frequencies minus equiluminant blank control. Frequencies are *A*, 0.5 Hz; *B*, 1 Hz; *C*, 4 Hz; *D*, 8 Hz, and *E*, 16 Hz. Percent signal change for the 5 maps is shown below panels *B* and *C*. A superpixel placed within a luminance-change domain within V2 is indicated with a small box in each of the maps. In *F*, the signal strength (% change in reflectance) from this superpixel for each of the 5 temporal frequencies is shown following 5 s of stimulation. The camera frame shown in *A–E* is 8 × 8 mm. Scale bar: 1 mm.

most prominent in the 1 Hz (B) and 4 Hz (C) maps. To quantify the magnitude of response, a superpixel was placed within a luminance-change domain (small white square in panels A–E), and the signal strength at this point was measured after 5 s of stimulation. The graph shown in Figure 4*F* demonstrates the bias toward lower frequencies with the strongest signal change from a 1-Hz stimulus. Thus, consistent with our expectation, the locations of luminance activations were constant, modulations ranging from 0.5 to 16 Hz produced significant activations, and the optimal population response was somewhat lower than the optimal temporal frequencies of previously published single-unit studies (Levitt et al. 1994).

Luminance Modulation and Binocular Preference Response in V3

Although the aim of this study was to examine functional organization in V2, our procedures exposed cortex anterior to V2, which included the third visual area (V3). Like V2, V3 also demonstrated the presence of orientation preference domains. Orientation preference domains in V3 were grouped into large clusters. In some cases, 2 or more OR stripes in V2 were observed to merge into these larger clusters of orientation-responsive domains in V3 (see Figs 3*A*–6*A*). The larger clusters of orientation domains in V3 were often separated by much smaller gaps lacking OR preference domains (e.g., Fig. 3*A*, arrow). The gaps in V3 that failed to demonstrate OR domains were, in some cases, coextensive with regions of V2 lacking orientation preference domains. As such, some degree of continuity was evident from V2 to V3 with respect to both orientation preference domains and regions lacking orientation preference domains, as previously reported (Xu et al. 2004).

In every case where luminance-change domains were evident in V2, they were also apparent in V3. For example, 2 oval-shaped luminance-change domains were evident in V3 in case 07-37L (Fig. 4*B*, or light green shading, Fig. 4*E*). These were of similar size and shape to those observed in V2 in this case. In another case, 9 smaller oval-shaped luminance-change domains were observed in V3 (Fig. 5*B,D*). In this case, the V3 luminance-change domains were smaller than those in V2. In a third case (Fig. 6*B,E*), 3 luminance-change domains were apparent in V3. These domains in V3 were of similar size and shape to those in V2.

Binocular domains were apparent in V3 in each case examined. For example in Figure 4*C*, 2 prominent oval-shaped domains were visible in V3 and appeared "in line" with those in V2, giving the impression of binocular preferring stripes, that ran from V2 to V3. In this case, another larger irregularly shaped binocular domain was evident that appeared continuous across the V2/V3 border. Five binocular domains were observed in V3 in a second case, shown in Figure 5*C,D*. In this case, the binocular domains appeared to alternate with "monocularly-biased" regions in a zebra stripe-like fashion, indicated with a light gray oval in Figure 5*C*. In a third case, 4 binocular domains were observed in V3 (Fig. 6*C,E*). These domains were larger than those observed in other cases.

In V3, as in V2, the locations of luminance-change domains and binocular domains were related. In all cases examined, luminance-change domains and binocular domains in V3 occupied adjacent or nonoverlapping regions of cortex. These domains were never found to coincide with each other. For example, in Figure 4*E*, 2 luminance-change domains were observed adjacent to 2 similarly sized binocular domains. This same relationship was observed in another case (Fig. 5*C,D*), where luminance-change domains and binocular domains interdigitated with one another (see gray oval in Fig. 5*C*). In Figure 6*E*, binocular domains were observed next to luminance-change domains. In V2, luminance-change domains tended to interdigitate with regions containing orientation preference and binocular domains. In V3, large regions of orientation preference domains were apparent, but within these regions, both luminance-change domains and binocular domains were typically observed. Hence, in V3, luminance-change domains and binocular domains were nonoverlapping. As in V2, binocular domains tended to overly orientation domains. However, unlike V2, luminance-change domains were found overlying regions of orientation preference as well as regions lacking in orientation preference.

Discussion

In the present study, we used optical imaging to reveal aspects of the modular organization of areas V2 and V3 of New World owl monkeys. Monkeys are known to have 3 functionally distinct types of modules in V2, the so-called thick, thin, and pale stripes, named after their appearance in brain sections processed for CO. In macaque monkeys, the thick stripes are most highly activated when both eyes are stimulated (Chen et al. 2008), and present evidence indicates that this is the case for owl monkeys as well. In addition, the thin stripes in macaque monkeys are responsive to changes in luminance (Wang et al. 2007), and we have demonstrated that the thin stripes of owl monkeys also have this property. Thus, these and other properties of the modular organization of area V2 of anthropoid primates have been retained in 2 distinct lines of descent for at least 40 million years, even though owl monkeys became the only nocturnal monkey, having evolved from dichromatic diurnal New World monkey ancestors, whereas macaque monkeys are diurnal trichromatic Old World monkeys. The conservation of these features over such long periods of time and over a considerable divergence in other features of the visual system suggests that the modular organization of V2 in primates, once achieved, has been valuable enough to remain. Other characteristics of V2, such as the size of this area relative to the total size of the visual cortex, also seem to have remained relatively constant (Kaskan et al. 2005). Quite likely, these and other features of V2 of monkeys have been retained in humans. These and other aspects of the modular organization of V2 of owl monkeys are discussed and compared with other primates in more detail below. In addition, our evidence that area V3 of owl monkeys has orientation-selective, binocular and luminance-change domains is related to previous findings. Although optical imaging V3 has not been possible in macaques, where V3 is hidden deep in fissures, it has been possible to image modular features of V3 in New World owl monkeys (Lyon et al. 2002; Xu et al. 2004). However, the present report is the first to demonstrate modular activations in V3 related to luminance change or binocularity.

Orientation Selectivity and CO Architecture in Owl Monkey V2

To date, our understanding of the organization of V2 in owl monkeys comes from 2 lines of investigation. In owl monkeys, V2 was initially defined by microelectrode recordings (Allman and Kaas 1974) but was later characterized in sections flattened and stained for CO (Tootell et al. 1985). In these sections, CO-

dark stripes alternated with CO-light stripes and were oriented perpendicular to the V1/V2 border. CO-dark stripes were spaced about 1–1.5 mm apart, and some noticeably thicker stripes alternated with thin stripes. In the cases we examined, CO-dense regions were present in a surround of less heavily stained tissue, but not all cases exhibited "thick" and "thin" CO stripes. For instance in Figure 1, CO-dense stripes do not always cross the width of V2 and are similar in width. However, in another case (Fig. 4*D*), CO stripes are alternately thick and thin and run across the width of V2. Though we observed variability from case to case in the appearance of CO-dense regions, these regions were always present in V2. Moreover, CO-dense regions consistently corresponded to regions of V2 activated by particular kinds of stimuli. These stimuli were oriented gratings and gratings presented binocularly (to elicit binocular-biased activation) and full-field changes in luminance (to elicit activation related to luminance change).

Previous optical imaging studies of V2 in owl monkeys have examined the organization of orientation selectivity and correlated the locations of OR-selective stripes with the CO-dense thick stripes and neighboring pale stripes (Xu et al. 2004). In general, our data support these findings. In most cases, well-organized OR stripes were evident (e.g., see Figs 4*A* and 5*A*). In parallel to the variability of CO architecture that we observed, we found variability in patterns of orientation selectivity. Some cases exhibited well-organized OR stripes (see Figs 4*A* and 5*A*), but others were less "stripe-like" (Fig. 6*A*). Though orientation selectivity varied in its organization, patterns of CO expression paralleled this variability, such that the most "stripe-like" patterns of orientation selectivity were found in cases with prominent CO-thick and CO-thin stripes (see Fig. 4). In cases where OR stripes were not well organized or appeared jumbled, patterns of CO expression were likewise disorganized (Fig. 6). The variability in the extent and organization of orientation-selective domains is paralleled by variability in CO stripes. Others have also noted the variability of CO stripes in owl monkeys (Tootell et al. 1985). This variability is not surprising, given that CO is an enzyme associated with metabolic activity (Wong-Riley 1989). The variables that influence the development of processing modules in V2 also seem to influence patterns of CO expression, such that functionally related groups of cells in V2 have corresponding metabolic architectures revealed through CO expression. The CO thick and pale stripe organization and related orientation domains are clearly more variable in owl monkeys than in macaque monkeys (Tootell et al. 1989; Ts'o et al. 2001; Vanduffel et al. 2002; reviewed in Roe 2003 and Roe et al. 2007) or squirrel monkeys (Krubitzer and Kaas 1990a; Malach et al. 1994), where more regular relationships are observed from case to case. This difference may be a consequence of an adaptation to nocturnal life by owl monkeys.

Binocular Domains in Owl Monkey V2

The unique response profiles that disparity-selective neurons exhibit for different arrangements of receptive fields have been used to define different types of disparity-selective neurons in V2 in macaque monkeys (c.f., Poggio et al. 1988). Each type of disparity-selective neuron is maximally responsive when a stimulus falls upon both of its receptive fields but shows significantly reduced spike-firing rates when only one receptive field is stimulated. We used this difference in firing rate to identify the locations of cells that show greater responses to binocular stimulation than monocular stimulation, thereby identifying locations more likely to contain disparity-selective cells. The resulting patterns revealed regions of owl monkey V2 that exhibited greater activity to binocular stimulation than surrounding regions, and we termed these regions binocular preference domains. This study provides the first evidence of binocular preference domains in owl monkeys.

In macaque monkeys, binocular preference domains co-localize with the thick stripes of V2 (Ts'o et al. 2001), and binocular preference is believed to reflect the prominence of disparity-selective neurons in V2 thick stripes (Livingstone and Hubel 1987; Poggio et al. 1988; Peterhans and von der Heydt 1993; Roe and Ts'o 1995; Ts'o et al. 2001; Bakin et al. 2000). Indeed, a recent study has directly demonstrated the co-localization of binocular preference and maps for near-to-far disparity within the thick stripes of V2 in macaque monkeys (Chen et al. 2008), providing further evidence for a role of thick stripes in binocular integration. The correspondence shown in this study between binocular preference domains and thick stripes raises the possibility that thick stripes in owl monkeys are also regions of disparity selectivity, something that will require further investigation. Although binocular preference does not necessarily imply disparity selectivity, it is consistent with the presence of disparity-selective neurons. Though the owl monkeys in these experiments did not have a binocularly converged view of the screen, it is unlikely that this could have produced an artificial map of binocular preference for 2 reasons: 1) our findings were consistent from case to case, despite the fact that the each animal's eyes were in different locations on the screen; and 2) relative eye position effects the location of near and far disparity domains, not the location of binocular preference domains (Chen et al. 2008).

Our experiments demonstrated the presence of binocularly biased regions of V2 in owl monkeys and that these binocular domains overlapped regions of well-organized orientation selectivity. In cases where CO stripes appeared relatively thick and thin, binocular domains correlated with the locations of CO-thick stripes. In owl monkeys, as in macaque monkeys, binocular domains, OR-selective stripes and CO-thick stripes share common territories within V2.

In macaque monkeys, CO-dense thick stripes have reciprocal connections with the middle temporal visual area (MT) (Shipp and Zeki 1985; DeYoe and Van Essen 1985; Shipp and Zeki 1989). MT, one of the many proposed visual areas that is recognized as present in all primates (Kaas 1997), is a myelin and CO-dense area containing a high proportion of directionally selective and disparity-selective neurons (for review, see Orban 1997; Born and Bradley 2005). In macaque monkeys, the majority of V2 connections with MT are with regions characterized as CO-thick stripes. These connections may be crucial for relaying signals related to disparity to the dorsal stream area MT, where columns of disparity-selective cells have been hypothesized to be present (DeAngelis and Newsome 1999). Consistent with this hypothesis, inactivation by cooling of V2 and the neighboring visual area V3 degrades the disparity tuning curves of binocular neurons in MT (Ponce et al. 2008). In some studies of smaller New World monkeys, where it has been difficult to tell thick from thin, it has been difficult to discern which type of CO-dense stripes have connections with MT (Krubitzer and Kaas 1990a). Nevertheless, in these studies, modular patterns of connectivity are clearly evident between MT and V2. Our study is consistent with the role of thick

stripes in dorsal pathway function. However, combined optical imaging and tracer studies in owl monkeys are needed to directly establish the association between MT and regions of binocular integration in V2.

Luminance-Change Domains in Owl Monkey V2

We were able to activate regions of V2 in owl monkeys using sinusoidally modulated wide-field luminance or stimuli containing abrupt changes in luminance. This is the first report of luminance-change domains in V2 of owl monkeys. In general, these regions did not overlap with those activated by oriented gratings and binocular stimulation. In optical imaging maps of orientation or binocular preference, we typically found spaces or gaps in the map. By correlating orientation or binocular preference maps to patterns of activation elicited by changes in luminance, we discovered that the spaces or gaps in maps of orientation and binocular preference corresponded to the locations of cortex activated by luminance modulation. Furthermore, we discovered that luminance-change domains correlated to CO-dense stripes or spots. In some cases, we were able to identify these CO-dense regions as thin stripes. In other cases, the stripes appeared dense but did not seem to be thicker or thinner than neighboring CO-dense regions. In these cases, the prominent "stripe-like" CO architecture was not present, and V2 appeared as a jumbled collection of CO-dense ovals or stripes.

To date, there have been no studies on the functional properties of cells associated with CO-thin stripes in owl monkeys. In macaque monkeys, thin stripes are associated with the processing of surface features such as color and luminance (Hubel and Livingstone 1987; Xiao et al. 2003; Wang et al. 2007; Roe et al. 2005a; Lu et al. 2007). Optical imaging studies have demonstrated the presence of hue maps (Xiao et al. 2003; Roe et al. 2007) and achromatic luminance domains (Roe and Ts'o 1995, Ts'o et al. 2001, Wang et al. 2007) within V2 thin stripes of macaque monkeys). These maps contain domains of color- or achromatic-luminance preference. Furthermore, thin stripes exhibit responsiveness to both luminance and perceived brightness change (Roe et al. 2005a) and with greater dynamic range of contrast sensitivity (Lu et al. 2007), consistent with a preferential role in surface feature encoding. Because owl monkeys express only one type of cone in the retina, the medium wavelength or M-cone (Wikler and Rakic 1990; Jacobs et al. 1993, 1996), we focused on achromatic stimuli containing only luminance change. Our findings suggest that thin stripes in owl monkeys may share similar role of processing surface feature information.

Luminance provides a basic cue to the percept of brightness, an attribute commonly ascribed to surfaces and the ventral stream. Cells responsive to full-field stimulation and changes in luminance may be involved in representing surfaces. Electrophysiological and optical imaging experiments have provided evidence for the presence of such cells in V1 (Bartlett and Doty 1974; Kayama et al. 1979; Maguire and Baizer 1982; Rossi et al. 1996; Kinoshita and Komatsu 2001; Peng and Van Essen 2005; Roe et al. 2005; Tucker and Fitzpatrick 2006; Geisler et al. 2007; Hung et al. 2007). Less is known about luminance-responsive cells in V2, but what is known suggests that these cells are present in V2 and are associated with CO-thin stripes in macaque monkeys (Roe et al. 2005a; Wang et al. 2007; Roe and Ts'o 1995; Ts'o et al. 2001). This literature suggests that thin stripes in owl monkeys may be involved in processing luminance, and our data support this conclusion. We have identified patterns of visually evoked activation in response to luminance change that correspond to the locations of CO-dense stripes that typically can be identified as "thin."

V2 Comparisons with Other Primates—Similarities and Differences

The majority of optical imaging studies have been carried out in macaque monkeys, but some studies have investigated V2 organization in marmosets (Roe et al. 2005b; McLaughlin and Schiessl 2006), owl monkeys (Xu et al. 2004), and squirrel monkeys (Malach et al. 1994). In species other than macaque monkeys, the organization of orientation selectivity has been the focus, and in general, regions of orientation selectivity are organized in stripes or patches that stretch across the anterior-posterior extent of V2. For instance, in squirrel monkeys, highly selective regions of orientation preference are centered on CO-thick stripes, but orientation preference domains also involve CO-pale stripes (Malach et al. 1994). In owl monkeys and marmosets, the "stripe-like" organization of orientation selectivity has been reported previously, and, as in squirrel monkeys regions of orientation selectivity are centered over CO-thick stripes, but also "spread" into neighboring CO-pale regions (Xu et al. 2004; Roe et al. 2005b; McLaughlin and Schiessl 2006). We have also observed CO-pale regions to exhibit orientation selectivity that seems continuous with that associated with neighboring CO-thick stripes.

Our experiments on V2 of owl monkeys indicate that luminance change regions correspond to gaps between orientation preference regions and to the locations of CO-dense stripes or spots, which in some cases appear thinner than neighboring CO-thick stripes. The luminance-change domains and neighboring binocular domains that we describe here have not been reported in other studies of New World monkeys. Hence, we can only relate this data to what is known about these functional modules in macaque monkeys, where domains biased to respond to binocular stimulation correspond to CO-thick stripes (Ts'o et al. 2001; Chen et al. 2008) and luminance-change domains correspond to thin CO stripes (Wang et al. 2007). We find the same spatial relationships in New World owl monkeys, which have not shared a common ancestor with Old World macaque monkeys in about 40 million years. Despite the fact that these 2 primates are distantly related and have evolved on separate continents to occupy nocturnal or diurnal niches, the organization of V2 is similar in the 2 primates, although the shapes and sizes of domains are more variable across individuals in owl monkeys.

Orientation-Preference, Binocular Domains, and Luminance-Change Domains in V3

V3 is an area along the outer border of V2 that is similar in shape but more narrow than V2; V3 mirrors V2 in retinotopy (for review, see Kaas and Lyon 2001). In prosimians (Lyon and Kaas 2002b), New World marmosets, owl monkeys and titi monkeys (Lyon and Kaas 2002a), and macaque monkeys (Lyon and Kaas 2002c), V3 has separate dorsal and ventral halves along the outer margin of V2 that are similar in architecture and connections. Optical imaging experiments have verified the size and location of dorsal V3 in owl monkeys (Lyon et al. 2002). Thus, there is considerable evidence that the luminance-

change domains and binocular domains we observed anterior to V2 were indeed in V3.

This is the first study to reveal patterns of visually evoked activation in V3 related to luminance or binocularity. Previous studies of the response properties of neurons in V3 in macaque monkeys have identified cells responsive to luminance, orientation, and binocular disparity (Felleman and Van Essen 1987; Gegenfurtner et al. 1997). However, little is known about their functional organization. We found no clear relationship between functional domains in V3 and patterns of CO expression in V3, which were quite irregular.

As previously reported (Xu et al. 2004), orientation domains in V3 form bands that are much wider than those in V2. However, luminance-change domains and binocular domains in V3 were similar in size and shape to those in V2. As in V2, in V3, luminance-change domains and binocular domains occupied adjacent regions of cortex; these domains were never found in coregistration, suggesting segregated pathways to and from V3 related to luminance or binocularity, yet luminance-change domains in V3 differed from those in V2 in that they were located in regions of V3 where orientation preference domains were found. Orientation preference domains in V3 were coextensive, in some regions, with luminance-change domains, and in others, with binocular domains, suggesting that V3 is involved with integrating luminance and orientation, and binocularity and orientation. Further study will be required to examine the role of V3 in higher order perceptual processes requiring the integration of information about orientation, luminance and binocularity.

Supplementary Material

Supplementary figures can be found at http://www.cercor.oxfordjournals.org.

Funding

National Eye Institute Grants EY002686 (to J.H.K.), EY11744 (to A.W.R.), and T32 EY007135 (to P.M.K.).

Notes

We would like to thank Haidong Lu for writing analysis code and Dan Shima for stimulus generation code. We would also like to thank Mary Baldwin and Reuben Fan for their help during experiments. *Conflict of Interest:* None declared.

Address correspondence to Peter M. Kaskan, Department of Psychology, Vanderbilt University, 301 Wilson Hall, 111 21st Avenue South, Nashville, TN 37203, USA. Email: peter.m.kaskan@vanderbilt.edu.

References

Adams DL, Horton JC. 2003. Capricious expression of cortical columns in the primate brain. Nat Neurosci. 6(2):113–114.

Allman JM, Kaas JH. 1974. The organization of the second visual area (V II) in the owl monkey: a second order transformation of the visual hemifield. Brain Res. 76(2):247–265.

Bakin JS, Nakayama K, Gilbert CD. 2000. Visual responses in monkey areas V1 and V2 to three-dimensional surface configurations. J Neurosci. 20:8188–8198.

Bartlett JR, Doty RW, Sr. 1974. Response of units in striate cortex of squirrel monkeys to visual and electrical stimuli. J Neurophysiol. 37(4):621–641.

Born RT, Bradley DC. 2005. Structure and function of visual area MT. Annu Rev Neurosci. 28:157–189.

Casagrande V, Kaas J. 1994. The afferent, intrinsic, and efferent connections of primary visual cortex in primates. In: Peters A, Rockland K, editors. Cerebral Cortex, Vol. 10: Primary visual cortex in primates. New York: Plenum Press. p. 201–259.

Chen G, Lu HD, Roe AW. 2008. A map for horizontal disparity in monkey V2. Neuron. 58:442–450.

Constantine-Paton M, Law MI. 1978. Eye-specific termination bands in tecta of three-eyed frogs. Science. 202(4368):639–641.

DeAngelis GC, Newsome WT. 1999. Organization of disparity-selective neurons in macaque area MT. J Neurosci. 19:1398–1415.

DeYoe EA, Van Essen DC. 1985. Segregation of efferent connections and receptive field properties in visual area V2 of the macaque. Nature. 317(6032):58–61.

DeYoe EA, Van Essen DC. 1988. Concurrent processing streams in monkey visual cortex. Trends Neurosci. 11(5):219–226.

Felleman DJ, Van Essen DC. 1987. Receptive field properties of neurons in area V3 of macaque monkey extrastriate cortex. J Neurophysiol. 57(4):889–920.

Felleman DJ, Xiao Y, McClendon E. 1997. Modular organization of occipito-temporal pathways: cortical connections between visual area 4 and visual area 2 and posterior inferotemporal ventral area in macaque monkeys. J Neurosci. 17(9):3185–3200.

Florence SL, Kaas JH. 1992. Ocular dominance columns in area 17 of Old World macaque and talapoin monkeys: complete reconstructions and quantitative analyses. Vis Neurosci. 8(5):449–462.

Gattass R, Sousa AP, Mishkin M, Ungerleider LG. 1997. Cortical projections of area V2 in the macaque. Cereb Cortex. 7(2):110–129.

Gegenfurtner KR, Kiper DC, Fenstemaker SB. 1996. Processing of color, form, and motion in macaque area V2. Vis Neurosci. 13(1):161–172.

Gegenfurtner KR, Kiper DC, Levitt JB. 1997. Functional properties of neurons in macaque area V3. J Neurophysiol. 77(4):1906–1923.

Geisler WS, Albrecht DG, Crane AM. 2007. Responses of neurons in primary visual cortex to transient changes in local contrast and luminance. J Neurosci. 27(19):5063–5067.

Horton JC. 1984. Cytochrome oxidase patches: a new cytoarchitectonic feature of monkey visual cortex. Philos Trans R Soc Lond B Biol Sci. 304:199–253.

Horton JC, Hocking DR. 1996. Intrinsic variability of ocular dominance column periodicity in normal macaque monkeys. J Neurosci. 16(22):7228–7239.

Hubel DH, Livingstone MS. 1985. Complex-unoriented cells in a subregion of primate area 18. Nature. 315(6017):325–327.

Hubel DH, Livingstone MS. 1987. Segregation of form, color, and stereopsis in primate area 18. J Neurosci. 7:3378–3415.

Hung CP, Ramsden BM, Roe AW. 2007. A functional circuitry for edge-induced brightness perception. Nat Neurosci. 10(9):1185–1190.

Jacobs GH, Tootell RB, Blakeslee B. 1979. Visual capacities of the owl monkey (*Aotus trivirgatus*): temporal contrast sensitivity. Folia Primatol. 32(3):193–199.

Jacobs GH, Deegan JF, 2nd, Neitz J, Crognale MA, Neitz M. 1993. Photopigments and color vision in the nocturnal monkey, *Aotus*. Vision Res. 33(13):1773–1783.

Jacobs GH, Neitz M, Neitz J. 1996. Mutations in S-cone pigment genes and the absence of colour vision in two species of nocturnal primate. Proc Biol Sci. 263(1371):705–710.

Jones DG, Van Sluyters RC, Murphy KM. 1991. A computational model for the overall pattern of ocular dominance. J Neurosci. 11(12):3794–3808.

Kaas JH. 1997. Theories of visual cortex organization in primates. In: Rockland KS, Kaas JH, Peters A, editors. Cerebral Cortex: extrastriate cortex in primates. New York: Plenum. p. 91–125.

Kaas JH, Lyon DC. 2001. Visual cortex organization in primates: theories of V3 and adjoining visual areas. Prog Brain Res. 134:285–295.

Kaas JH, Catania KC. 2002. How do features of sensory representations develop? Bioessays. 24(4):334–343.

Kaskan PM, Franco EC, Yamada ES, Silveira LC, Darlington RB, Finlay BL. 2005. Peripheral variability and central constancy in mammalian visual system evolution. Proc Biol Sci. 272:91–100.

Kaskan PM, Lu HD, Dillenburger BC, Roe AW, Kaas JH. 2007. Intrinsic-signal optical imaging reveals cryptic ocular dominance columns in primary visual cortex of New World owl monkeys. Front Neurosci. 1(1):67–75.

Kayama Y, Riso RR, Bartlett JR, Doty RW. 1979. Luxotonic responses of units in macaque striate cortex. J Neurophysiol. 42(6):1495–1517.
Kinoshita M, Komatsu H. 2001. Neural representation of the luminance and brightness of a uniform surface in the macaque primary visual cortex. J Neurophysiol. 86(5):2559–2570.
Krubitzer LA, Kaas JH. 1989. Cortical integration of parallel pathways in the visual system of primates. Brain Res. 478(1):161–165.
Krubitzer LA, Kaas JH. 1990a. Cortical connections of MT in four species of primates: areal, modular, and retinotopic patterns. Vis Neurosci. 5(2):165–204.
Krubitzer LA, Kaas JH. 1990b. Convergence of processing channels in the extrastriate cortex of monkeys. Vis Neurosci. 5(6):609–613.
LeVay S, Connolly M, Houde J, Van Essen DC. 1985. The complete pattern of ocular dominance stripes in the striate cortex and visual field of the macaque monkey. J Neurosci. 5(2):486–501.
Levitt JB, Kiper DC, Movshon JA. 1994. Receptive fields and functional architecture of macaque V2. J Neurophysiol. 71(6):2517–2542.
Livingstone MS, Hubel DH. 1982. Thalamic inputs to cytochrome oxidase-rich regions in monkey visual cortex. Proc Natl Acad Sci U S A. 79: 6098–6101.
Livingstone MS, Hubel DH. 1983. Specificity of cortico-cortical connections in monkey visual system. Nature. 304:531–534.
Livingstone MS, Hubel DH. 1987. Psychophysical evidence for separate channels for the perception of form, color, movement, and depth. J Neurosci. 7(11):3416–3468.
Livingstone MS, Hubel DH. 1988. Segregation of form, color, movement, and depth: anatomy, physiology, and perception. Science. 240(4853):740–749.
Lu HD, Roe AW. 2007. Optical Imaging of Contrast Response in Macaque Monkey V1 and V2. Cereb Cortex. 17:2675–2695.
Lyon DC, Kaas JH. 2002a. Evidence from V1 connections for both dorsal and ventral subdivisions of V3 in three species of New World monkeys. J Comp Neurol. 449(3):281–297.
Lyon DC, Kaas JH. 2002b. Connectional evidence for dorsal and ventral V3, and other extrastriate areas in the prosimian primate, *Galago garnetti*. Brain Behav Evol. 59(3):114–129.
Lyon DC, Kaas JH. 2002c. Evidence for a modified V3 with dorsal and ventral halves in macaque monkeys. Neuron. 33(3):453–461.
Lyon DC, Xu X, Casagrande VA, Stefansic JD, Shima D, Kaas JH. 2002. Optical imaging reveals retinotopic organization of dorsal V3 in New World owl monkeys. Proc Natl Acad Sci USA. 99(24): 15735–15742.
Maguire WM, Baizer JS. 1982. Luminance coding of briefly presented stimuli in area 17 of the rhesus monkey. J Neurophysiol. 47(1):128–137.
Malach R. 1994. Cortical columns as devices for maximizing neuronal diversity. Trends Neurosci. 17(3):101–104.
Malach R, Tootell RB, Malonek D. 1994. Relationship between orientation domains, cytochrome oxidase stripes, and intrinsic horizontal connections in squirrel monkey area V2. Cereb Cortex. 4(2):151–165.
McLoughlin N, Schiessl I. 2006. Orientation selectivity in the common marmoset (*Callithrix jacchus*): the periodicity of orientation columns in V1 and V2. Neuroimage. 31:76–85.
Nakagama H, Tanaka S. 2004. Self-organization model of cytochrome oxidase blobs and ocular dominance columns in the primary visual cortex. Cereb Cortex. 14(4):376–386.
Nascimento-Silva S, Gattass R, Fiorani M, Jr, Sousa AP. 2003. Three streams of visual information processing in V2 of Cebus monkey. J Comp Neurol. 466(1):104–118.
O'Keefe LP, Levitt JB, Kiper DC, Shapley RM, Movshon JA. 1998. Functional organization of owl monkey lateral geniculate nucleus and visual cortex. J Neurophysiol. 80(2):594–609.
Olavarria JF, Van Essen DC. 1997. The global pattern of cytochrome oxidase stripes in visual area V2 of the macaque monkey. Cereb Cortex. 7(5):395–404.
Orban G. 1997. Visual processing in macaque area MT/V5 and its satellites (MTSd and MSTv). In: Rockland KS, Kaas JH, Peters A, editors. Cerebral Cortex: extrastriate cortex in primates. New York: Plenum. p. 91–125.
Peng X, Van Essen DC. 2005. Peaked encoding of relative luminance in macaque areas V1 and V2. J Neurophysiol. 93(3):1620–1632.
Penn AA, Riquelme PA, Feller MB, Shatz CJ. 1998. Competition in retinogeniculate patterning driven by spontaneous activity. Science. 279(5359):2108–2112.
Peterhans E, von der Heydt R. 1993. Functional organization of area V2 in the alert macaque. Eur J Neurosci. 5(5):509–524.
Poggio GF, Gonzalez F, Krause F. 1988. Stereoscopic mechanisms in monkey visual cortex: binocular correlation and disparity selectivity. J Neurosci. 8(12):4531–4550.
Ponce CR, Lomber SG, Born RT. 2008. Integrating motion and depth via parallel pathways. Nat Neurosci. 11(2):216–223.
Ramsden BM, Hung CP, Roe AW. 2001. Real and illusory contour processing in area V1 of the primate: a cortical balancing act. Cereb Cortex. 11(7):648–665.
Roe AW, Ts'o DY. 1995. Visual topography in primate V2: multiple representation across functional stripes. J Neurosci. 15(5 Pt 2):3689–3715.
Roe AW, Ts'o DY. 1997. The functional architecture of area V2 in the Macaque monkey. In: Rockland K, Kaas JH, Peters A, editors. Cerebral Cortex, Vol. 12: extrastriate cortex in primates. New York: Plenum Press. p. 295–333.
Roe AW. 2003. Modular complexity of area V2 in the macaque monkey. In: Collins CE, Kaas JH, editors. The primate visual system. New York: CRC Press. p. 109–138.
Roe AW, Lu HD, Hung CP. 2005. Cortical processing of a brightness illusion. Proc Natl Acad Sci USA. 1.2:3869–3874.
Roe AW, Lu HD, Hung CP. 2005a. Cortical processing of a brightness illusion. Proc Natl Acad Sci USA. 102:3869–3874.
Roe AW, Fritsches K, Pettigrew JD. 2005b. Optical imaging of functional organization of V1 and V2 in marmoset visual cortex. Anat Rec A Discov Mol Cell Evol Biol. 287(2):1213–1225.
Roe AW, Chen G, Lu HD. 2007. Functional architecture of area V2. In: Squire L, editor. Encyclopedia of neuroscience. Oxford (UK): Elsevier.
Rosa MG, Krubitzer LA. 1999. The evolution of visual cortex: where is V2? Trends Neurosci. 22:242–248.
Rossi AF, Rittenhouse CD, Paradiso MA. 1996. The representation of brightness in primary visual cortex. Science. 273(5278):1104–1107.
Shipp S, Zeki S. 1985. Segregation of pathways leading from area V2 to areas V4 and V5 of macaque monkey visual cortex. Nature. 315(6017):322–325.
Shipp S, Zeki S. 1989. The organization of connections between areas V5 and V2 in macaque monkey visual cortex. Eur J Neurosci. 1(4): 333–354.
Sincich LC, Horton JC. 2002. Divided by cytochrome oxidase: a map of the projections from V1 to V2 in macaques. Science. 295(5560): 1734–1737.
Sincich LC, Adams DL, Horton JC. 2003. Complete flatmounting of the macaque cerebral cortex. Vis Neurosci. 20(6):663–686.
Sincich LC, Horton JC. 2003. Independent projection streams from macaque striate cortex to the second visual area and middle temporal area. J Neurosci. 23(13):5684–5692.
Sincich LC, Horton JC. 2005. The circuitry of V1 and V2: integration of color, form, and motion. Annu Rev Neurosci. 28:303–326.
Stepniewska I, Kaas JH. 1996. Topographic patterns of V2 cortical connections in macaque monkeys. J Comp Neurol. 371(1):129–152.
Swindale NV. 1980. A model for the formation of ocular dominance stripes. Proc R Soc Lond B Biol Sci. 208(1171):243–264.
Tootell RB, Hamilton SL. 1989. Functional anatomy of the second visual area (V2) in the macaque. J Neurosci. 9:2620–2644.
Tootell RB, Hamilton SL, Silverman MS. 1985. Topography of cytochrome oxidase activity in owl monkey cortex. J Neurosci. 5(10): 2786–2800.
Tootell RB, Silverman MS, De Valois RL, Jacobs GH. 1983. Functional organization of the second cortical visual area in primates. Science. 220(4598):737–739.
Ts'o DY, Roe AW, Gilbert CD. 2001. A hierarchy of the functional organization for color, form and disparity in primate visual area V2. Vision Res. 41(10–11):1333–1349.
Tucker TR, Fitzpatrick D. 2006. Luminance-evoked inhibition in primary visual cortex: a transient veto of simultaneous and ongoing response. J Neurosci. 26(52):13537–13547.

Vanduffel W, Tootell RB, Schoups AA, Orban GA. 2002. The organization of orientation selectivity throughout macaque visual cortex. Cereb Cortex. 12(6):647–662.
Wang Y, Xiao Y, Felleman DJ. 2007. V2 thin stripes contain spatially organized representations of achromatic luminance change. Cereb Cortex. 17(1):116–129.
Wikler KC, Rakic P. 1990. Distribution of photoreceptor subtypes in the retina of diurnal and nocturnal primates. J Neurosci. 10(10):3390–3401.
Wong-Riley MT. 1979. Changes in the visual system of monocularly sutured or enucleated cats demonstrable with cytochrome oxidase histochemistry. Brain Res. 171:11–28.
Wong-Riley MT. 1989. Cytochrome oxidase: an endogenous metabolic marker for neuronal activity. Trends Neurosci. 12(3):94–101.
Wright P. 1994. Night watch on the Amazon. Nat Hist. 103:44–52.
Xiao Y, Zych A, Felleman DJ. 1999. Segregation and convergence of functionally defined V2 thin stripe and interstripe compartment projections to area V4 of macaques. Cereb Cortex. 9(8): 792–804.
Xiao Y, Wang Y, Felleman DJ. 2003. A spatially organized representation of colour in macaque cortical area V2. Nature. 421(6922):535–539.
Xiao Y, Felleman DJ. 2004. Projections from primary visual cortex to cytochrome oxidase thin stripes and interstripes of macaque visual area 2. Proc Natl Acad Sci USA. 101(18):7147–7151.
Xu X, Bosking W, Sary G, Stefansic J, Shima D, Casagrande V. 2004. Functional organization of visual cortex in the owl monkey. J Neurosci. 24(28):6237–6247.